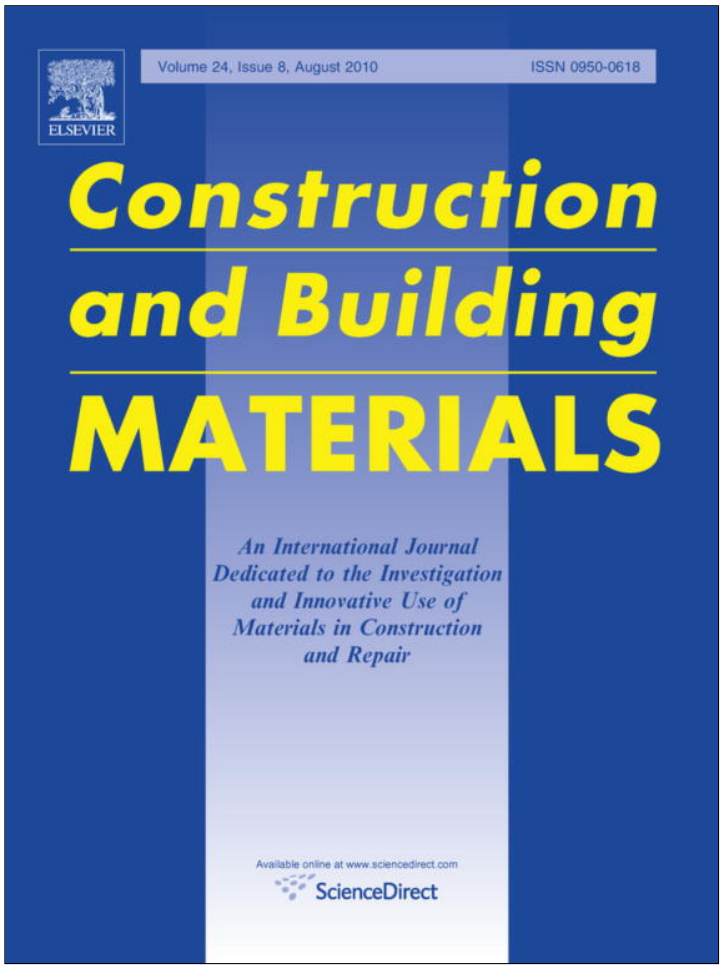

Construction and Building Materials 24 (2010) 1438–1448

Contents lists available at ScienceDirect

Construction and Building Materials

journal homepage: www.elsevier.com/locate/conbuildmat

Rough and polished travertine building stone decay evaluated by a marine aerosol ageing test

Maja Urosevic, Eduardo Sebastián-Pardo, Carolina Cardell *

Department of Mineralogy and Petrology, Faculty of Science, University of Granada, Campus Fuentenueva s/n, 18071 Granada, Spain

ARTICLE INFO

Article history:
Received 17 April 2009
Received in revised form 14 January 2010
Accepted 15 January 2010
Available online 4 February 2010

Keywords:
Travertine
Stone finishing processes
Marine aerosol
Ageing test
Pore system
Colourimetric features

ABSTRACT

Tablets of rough and polished travertine were aged in a sea-salt spray corrosion chamber to explore potentially contrasting stone decay behaviour due to different surface finishing processes. This paper presents a multianalytical approach to characterise the chemical, mineralogical, textural, porosimetric and colourimetric features of quarried and weathered travertine after the test. Rough and polished stone surfaces behave differently according to salt-spray absorption, newly formed pore networks, composition and habits of salts, and chromatic changes. Roughness and irregularities of the unpolished travertine favour salt inputs that in turn increase the open porosity. By contrast, the smooth finish of the polished travertine helps to protect it against salt decay, since this finishing blocks the pore system in the near-surface stone. This information is crucial to establish maintenance and conservation construction practices.

1. Introduction

For the goal of detecting and preventing salt deterioration on construction materials placed in architectural heritage, civil constructions and in present-day buildings, it is crucial to improve knowledge concerning weathering mechanisms involved in salt damage. Salt-induced deterioration of natural and artificial building materials (e.g. stones, mortars, bricks and ceramics) is drastically accelerated in coastal areas due to the action of marine aerosols, with significant cultural and economic implications [1–4]. In fact, the sizeable investment to preserve the architectural heritage, as well as to repair damage on ornamental and building materials used in modern constructions, makes necessary application of scientific knowledge due to salt weathering processes. Despite the abundant literature concerning this topic [5,6], little attention has been paid to ascertain the effect of different stone surface finishing processes to mitigate stone decay caused by marine aerosols.

In this regard great advances have been achieved as result of investigations conducted in the field of Heritage Science. In particular, laboratory tests have helped to shed light on causes and mechanisms involved in salt weathering of construction materials, as well as to allow easier recognition of key factors that trigger or mitigate their damage [1,7–12]. Though there are diverse international standard salt crystallisation tests (ASTM B-117 [13], DIN 50021 [14], ISO 9227 [15] and UNE-EN 14147 [16]), researchers have frequently designed *ad hoc* salt corrosion tests in an attempt to reproduce more realistic environmental conditions for better understanding the synergistic action of factors causing salt decay in construction materials. Thus different environmental conditions and solutions, as pure NaCl solutions [11,17], mixed solutions [9,17–19] or seawater spray [8,11] have been tested. In order to create a more realistic atmosphere for building stone decay in marine environments, a modified standard sea-salt spray test has been used in the present study to investigate the susceptibility of polished and rough surfaces of travertine stone samples due to the impact of marine aerosols.

Travertine has been an important building material for monuments and civil constructions from Roman times until present throughout Europe and near east [20–22]. It has been used as structural stone (ashlars and plane surfaces) and also in ornamental elements such as sculptures. In fact, travertine is one of the most frequently used stones in modern architecture worldwide, and is commonly seen in tile sizes as façade material, wall cladding, and flooring (for instance modern buildings such as the Getty Center in Los Angeles and Barcelona's Prat airport are cladded with travertine). Despite its widespread use, travertine has been investigated less than other carbonate stones like marbles and limestones, particularly in Andalusia (Southern Spain) where local travertines have been used in numerous monuments [17,23], and in public buildings at present times.

Travertine stone is a natural chemical precipitate of carbonate minerals deposited from the water of mineral springs saturated

* Corresponding author. Tel.: +34 958242725; fax: +34 958243368.
E-mail address: cardell@ugr.es (C. Cardell).

0950-0618/$ - see front matter © 2010 Elsevier Ltd. All rights reserved.
doi:10.1016/j.conbuildmat.2010.01.011

with dissolved calcium bicarbonate [24]. As a consequence, the stone is characterised in general by pitted holes in its surface. However various types of travertine exist due to variation in depositional environment and components. Two broad lithotypes are porous travertine with large irregular pores, and the less porous massive travertine. In this work the studied *Olivillo* travertine belongs to this latter group. Since travertine can have many nooks and crannies, it can be effectively polished to a smooth, shiny finish (honed travertine) or unpolished, as well as unfilled or filled with different polymer and cement-based materials [25].

Physical properties and compositional characteristics of travertine have been studied in naturally weathered travertine buildings to investigate their response to diverse atmospheric conditions [26,27]. However laboratory analyses and tests of physical and chemical weathering of travertine remain scarce. Thus, there are still interesting open questions to be investigated, such as the effects of different finishing processes in travertine stone buildings on marine aerosols absorption.

This paper presents a laboratory ageing test using marine spray in a controlled-atmosphere chamber to examine the implications of rough and polished travertine stone surfaces on their salt decay. The degree of salt damage was estimated by comparing changes in mineralogical and chemical composition, petrophysical characteristics and chromatic variations between freshly quarried and aged samples. The results obtained have significance for the design of proper processing, protection, maintenance and intervention protocols for civil and historic buildings.

2. Materials and methods

2.1. Stone material

This research focuses on a travertine type currently used as building stone extracted in Andalusia (Almería province, Southern Spain). Relatively large travertine formations outcrop (>5 km^2) near the villages *Alhama de Almería* and *Alicún* [28]. This formation was deposited in perched springline and fluvio-lacustrine environments and later affected locally by subaerial exposure process [29,30]. Travertines are exploited in several quarries and commercialised as *Olivillo travertine* (hereafter referred as AL travertine), commonly used as building stone in modern architecture as well as stone restoration in the Granada (Southern Spain) cultural heritage [17,23].

The sawing direction of the selected material was perpendicular to the layering (vein cut). Two finishing surface types of AL travertine are commercialised, namely as rough surface and polished surface. Polished travertine is treated before the polishing process in order to increase its strength. This treatment consists of a two-step process where large pores are first filled with a beige coloured gypsum-based plaster, and then the surface is dressed with an epoxy silicone mixed resin. After the strengthening, the surface of the travertine tiles is finally polished.

In this work, two sets of travertine samples with rough and polished surfaces were cut as tablet samples (50 × 50 × 10 mm) for the sea-salt spray ageing test. Later on, stone samples were prepared according to the requirement of each analytical technique applied, as specified in Section 2.3.

2.2. Sea-salt spray ageing test

A saline spray chamber (CCONS series, INELTEC®) was used to investigate the effect of marine aerosol deposition on rough and polished travertine surfaces. To reproduce more realistic conditions of building stone decay in marine environment, seawater was collected from the Mediterranean Sea at Granada coast (Salobreña, Southern Spain), instead of using the standardised 5% solution of NaCl known as NSS (neutral salt spray) advised by international standards such as e.g. ASTM (B-117) [13], DIN (50021) [14], ISO 9227 [15] or UNE-EN (14147) [16]. However the NaCl concentration of these tests can differ (e.g. 10% or 20% NaCl) upon laboratory request.

Standard salt spray tests are widely used in the industrial sector including automotive, construction and aerospace industries to evaluate the corrosion resistance of finished surfaces or parts (coatings, metals, alloys, stones, etc.). These standards describe the essential procedures to perform each test specifying temperature, relative humidity, concentration and pH of the solution, air pressure of the sprayed solution, sample dimension, testing hours in NSS (e.g. 100 h in [13], 96 h in [15]), etc., which differ among the tests. The basic principle of long-term salt spray (fog) ageing tests consists of a continuous salt solution pulverisation (ASTM (B-117) [13]), although cycle tests are preferred to simulate ageing due to the cyclic nature of real environmental conditions. For example, the UNE-EN (14147) test [16] requires 60 cycles, each consisting of 4 h ± 15 min of salt spray (pH = 6.5–7.2) followed by 8 h ± 15 min of drying at 35 ± 5 °C.

Test requirements should be agreed between customer and laboratories or manufacturer. Test duration depends on the corrosion resistance of the studied material (e.g. construction stones); the more corrosion resistant the material, the longer the period needed to show signs of deterioration. Thus, testing periods range from a few hours (e.g. 8 or 24 h) to more than a month. Results can be represented as mass loss [16], although the usual ageing test criteria is the visual estimation of degradation, as salts precipitation, stone colour changes or other types of damages such as creation of fissures, cracks, pits, etc. Therefore at first it is difficult to predict the number of hours or cycles needed for a salt spray test, so generally a high number is chosen to ensure material degradation.

In this work, the travertine tablets were subjected to a modified UNE-EN (14147) ageing test [16] to re-create more realistic environmental conditions of coastal areas. Stone tablets were hung on a nylon thread from plastic bars inside the chamber so that all sample faces were exposed to the salt spray. Care was taken to avoid direct exposure of the samples to the salt spray atomizer. The chamber was electronically programmed to produce 160 cycles corresponding to 60 d. After this period the test was judged to have finalised since no significant further macroscopic changes were observed in the stones. Each cycle consisted of 3 h of seawater spray followed by 6 h of drying by forced air at 35 °C and relative humidity of 70 ± 2%. The chamber remained closed throughout the test, thus during the spray periods the relative humidity was higher (c.a. 98%). The composition of the seawater is shown in Table 1. Cations (Ca^{2+}, K^+, Na^+ and Mg^{2+}) were determined by means of inductively coupled plasma-atomic emission spectrometry (ICP-AES, Leeman Labs PS series) and anions (Cl^-, SO_4^{2-} and NO_3^-) by ion chromatography (IC, Dionex DX 300). The pH of the seawater was 7.84 at 20 °C (Eutech 1500). Water composition used in the present ageing test is relatively lower in chlorine, potassium and sodium compared to those used elsewhere whereas nitrate, sulphate and magnesium content is slightly higher [8,11]. Upon conclusion, travertine samples were removed from the chamber and analysed using various techniques.

2.3. Analytical techniques

The following methods and analytical techniques were used to characterise the pore filling in the polished stone, the freshly quarried travertine and to evaluate modifications induced by the test. Before and after the test the blocks were weighed. Throughout the test, macroscale observations and photographic records were made to assess the presence of efflorescences, evolution of crystalline habits, drying and decay of stone samples, as presented in Sections 3.3.1 and 3.3.2.

The mineralogical composition of the travertine, the stone pore filling and the crystallised efflorescences were determined by powder X-ray diffraction (XRD) using a Philips PW-1710 diffractometer equipped with an automatic slit window. For this aim, the samples were milled in an agate mortar to less than 50 μm particle size. Analysis conditions were: radiation Cu Kα (λ: 1.5405 Å), 40 kV voltage, 40 mA current intensity, explored area between 3° and 60° 2θ and goniometer speed of 0.01° 2θ/s. Automatic acquisition, evaluation and identification of minerals were performed by *Xpowder* software [31]. To identify the epoxy silicone resin composition, transmittance Fourier transform-infrared spectroscopy (T-FTIR) was applied. The T-FTIR spectrum registered from 3999 to 400 cm^{-1} with a resolution of 2 cm^{-1} and 200 scans, were collected using a NICOLET spectrometer 20SXB. The T-FTIR spectrum was obtained from KBr pellet prepared by uniformly mixing 5 mg of powdered sample with KBr (3 wt.%).

Major and trace elements of fresh travertine were analysed using a Bruker S4 Pioneer X-ray fluorescence spectrometer (XRF) with wavelength dispersion equipped with a goniometer that held analysing crystals (LIF200/PET/OVO-55) and Rh X-ray tube (60 kV, 150 mA). Semiquantitative scanning spectra were obtained using the software Spectraplus. Stone powder (~5 g) was blended with wax (Hoestch wax C micropowder Merck) using a 5100 SPEX Mixer/Mill. After that

Table 1
Sea-salt water composition (expressed in ppm) used in this artificial ageing test (Mediterranean Sea) and from the Atlantic Ocean at the coast of Galicia (Vigo, Northwest Spain [8]).

	This study	[8]
Cl^-	12,879	22,050
NO_3^-	72	50
SO_4^{2-}	2772	2713
Ca^{2+}	330	345
K^+	348.4	1020
Na^+	10,030	19,920
Mg^{2+}	1069	945
HPO_4^{2-}	–	28

–: Not measured.

each sample was uniformly deposited on a cellulose substrate contained in a 40 mm aluminium cup. Finally, the product was pressed at 10 ton (Mignon-S de Nannetti) to produce a pressed pellet (40 mm sample disc).

Petrographic characteristics of fresh and aged travertines presenting rough and polished surfaces were examined under optical microscopy (OM) using an Olympus BX-60 equipped with digital camera (Olympus DP10). To this aim polished thin sections were prepared with ethanol to avoid salt dissolution, and stained with red alizarin to differentiate calcite from dolomite (calcite tints to red while dolomite remains unstained). Chips of these stone samples were also analysed with an environmental scanning microscope (ESEM) to study the stone microtexture, as well as crystal habits and chemical composition of precipitated salts without disturbing their hydration state. No sample preparation is required for ESEM analysis [12]. A Phillips Quanta 400 was used applying 20 kV acceleration voltage, 1 nA probe current and working distance of 10 mm.

The travertine pore system was characterised by means of mercury intrusion porosimetry (MIP) and gas sorption isotherms (BET). Blocks c.a. 2 cm^3 of fresh and aged samples (containing salts) were dried in an oven during 24 h at 60 °C, and analysed on a Micromeritics Autopore III model 9410 porosimeter. In addition, aged samples (rough and polished surfaces) were washed in distilled water during one week after the ageing test, and studied by means of gas Ar sorption. The purpose of this procedure was to discern the binding or cementing effect of salts in the stone. In samples with less than 5 $m^2\,g^{-1}$ surface area, Ar sorption measurements are more realistic than using N_2, which usually yield excessively high values [32]. The Ar sorption isotherms were obtained at −196 °C on a Micromeritics Tristar 3000 under continuous adsorption conditions. Prior to measurement, samples were heated to 250 °C for 8 h and outgassed to 10^{-3} Torr using a Micromeritics Flowprep. The BET analysis was used to determine the total specific surface area [33,34]. The Barret–Joyner–Halenda (BJH) method was used to obtain pore size distribution curves, the pore volume and the mean pore size of the travertine samples [35]. The surface fractal dimension, D_S, was determined from adsorption data and used to characterise the surface roughness. The analysis of the gas sorption isotherm using a modified Frenkel–Halsey–Hill (FHH) theory [36] allows determination of surface fractal dimension from the slope (A) of the plot of Ln(V) vs. Ln[Ln(P/P_0)], where V is the adsorbed volume of gas, and P and P_0 are the actual and condensation gas pressures. When surface tension (or capillary condensation) effects are important, the relationship between A and D_S is $A = D_S - 3$. Capillary condensation is significant if $\delta = 3(1 + A) - 2 < 0$. The pressure range and therefore the thickness range of the adsorbed layer coverage revealed that we were dealing only with monolayer (since n = 1–2). This thickness range ensures that the determination of D_S is reliable [36].

Chromatic characteristics of rough and polished surface samples before and after the ageing test were determined using a Minolta CR 210 colorimeter, with 0° viewing angle and 50 mm diameter measuring area. The CIE 1976 chromatic scale was used to measure the parameters L^*, a^* and b^* [37].

3. Results and discussion

The results of the pore filling analysis in the polished travertine are presented first. Then, to facilitate the comprehension of this work, the results of freshly quarried samples that display both surface finishing (i.e. polished and rough samples) are presented first, followed by the results for the corresponding surfaces of the aged travertine samples. However, all the results (from rough and polished stones) are shown together in the figures and tables to avoid unnecessary repetitions and to facilitate understanding of the text.

3.1. Surface finishing treatment

The XRD analysis revealed that the beige coloured gypsum-based plaster was composed of ~67% quartz (SiO_2), ~31% calcite ($CaCO_3$) and <2% illite (a type of phyllosilicate or layered alumino-silicate). T-FTIR analysis of polymeric materials provides highly precise measurements that are widely interpretable in terms of chemical structure. Most common epoxy resins are produced from a reaction between epichlorohydrin and bisphenol-A to obtain a polymer. The T-FTIR spectrum of the epoxy silicone resin analysed in this work (Fig. 1.) is comparable to other epoxy silicone resins reported elsewhere [38]. Fig. 1 shows the carbonyl band at 1730 cm^{-1}, the C–H stretch at 2930 cm^{-1} and the C–H scissoring and bending at 1460 cm^{-1}. The characteristic band of hydroxyl group was identified at 3479 cm^{-1} and the presence of C–O bands was observed in the region between 1030 and 1295 cm^{-1}.

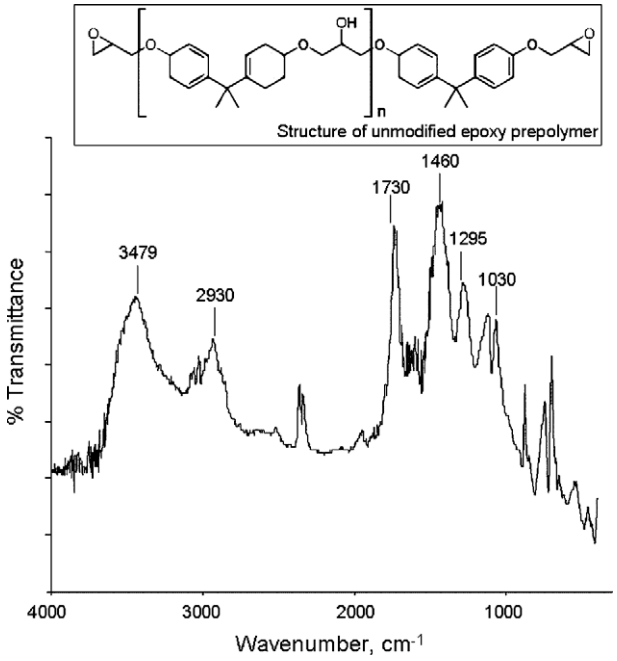

Fig. 1. T-FTIR spectrum of the epoxy silicone resin and its structure used in the finishing treatment of the polished travertine.

3.2. Fresh stone

3.2.1. Macroscale observations

The AL travertine is a massive travertine, mostly well cemented and heterogeneously coloured, varying from pale yellow to brown. It shows relatively small pores of c.a. 2–3 mm in size and larger ones at c.a. 20 mm. Also, a laminated structure is distinguished particularly when the material is polished, and the colour contrast of layers is enhanced (Fig. 2).

3.2.2. Bulk stone composition

The AL travertine bulk stone major composition and trace elements determined by XRF are presented in Table 2. Also for the purpose of comparison, chemical results from others travertine

Table 2
Representative major bulk stone composition and trace elements of *Olivillo* and *Alfacar* travertine (Granada, Southern Spain [17]) and mean values of some Italian travertines [39,40].

wt.%	*Olivillo*	*Alfacar*	Roman Travertine chiaro	Santa Sabina	Orvieto district	Cetona	Saturnia
SiO_2	0.96	1.93	0.68	1.75	8.69	5.23	0.05
TiO_2	0.02	–	–	0.02	0.10	0.08	*
Al_2O_3	0.32	0.44	0.54	0.54	2.52	1.94	0.08
Fe_2O_3	0.12	0.21	0.06	0.17	1.12	0.67	0.05
MnO	*	–	–	0.04	0.04	0.03	0.04
MgO	0.72	1.16	0.18	0.38	0.77	0.47	0.42
CaO	54.24	51.40	54.77	52.99	46.48	50.25	55.07
K_2O	0.06	0.10	–	0.11	0.59	0.27	*
P_2O_5	0.01	0.59	0.01	0.57	0.26	0.11	0.50
SO_3	0.19	–	0.45	–	–	–	–
Cl	0.01	–	–	–	–	–	–
ppm							
Cu	40	9	–	6	22	17	14
Zn	1000	49	–	11	31	34	6
Sr	1416	343	–	478	1546	826	749
Zr	55	<10	–	17	83	38	13

Detection limit is 0.005 wt.% for major elements and for trace elements 3 ppm for Zr, 2 ppm for Sr and 1 ppm for Cu, Zn, Zr. *: below detection limit, –: not measured.

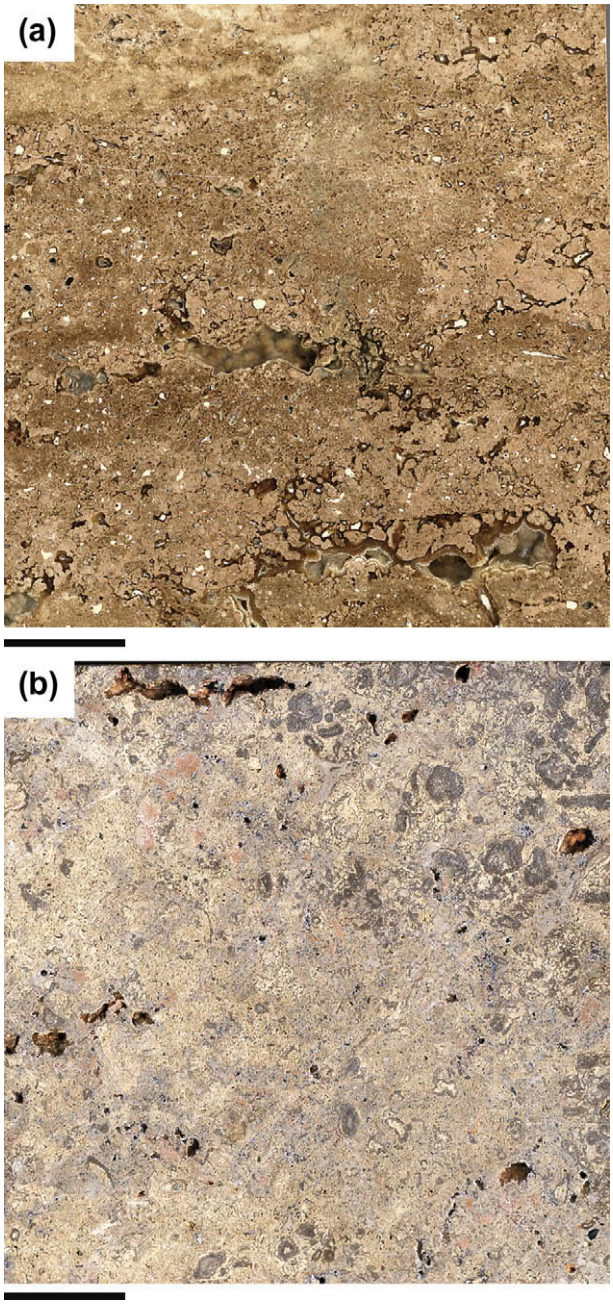

Fig. 2. Polished (a) and rough (b) surface of fresh *Olivillo* travertine. Note the porous laminated structure in (a). Bars = 10 mm.

lithotypes from Southern Spain and Italy are provided. AL travertine is low in siliciclastic components (i.e. SiO_2 and Al_2O_3) compared to other travertines (Table 2), being composed of almost pure calcite. Whereas the zirconium (Zr) value content is in the range of other travertines from Granada [17] and Italy [39,40], AL travertine is significantly enriched in copper (Cu) and zinc (Zn) and slightly in strontium (Sr). In the same locality (*Alhama de Almería*) iron (Fe) and manganese (Mn) oxides have been reported in another type of travertine displaying an intense red colour, known as *Red Alhama travertine*. However in this study MnO concentration was below detection limit of XRF. Contrasting depositional environment and different degrees of subaerial exposition (brecciation and karstification) have been noted in the same travertine formation exploited in several quarries [29]. Therefore the differences in MnO content and other minor elements measured can be ascribed to this heterogeneous distribution of facies and alterations.

3.2.3. Mineralogical and textural characteristics

The XRD data showed that calcite was the most abundant mineral in AL travertine (95–100%) with trace amounts (less than 5%) of quartz and phyllosilicates (illite-type). Detailed OM observations revealed that the lamination of AL travertine was related to changes in the ratio of sparitic (>10 μm in size) and microsparitic (4–10 μm)/micritic (<4 μm) calcite (Fig. 3). Higher proportion of the sparitic calcite leads to lighter band colour, vs. darker bands for higher proportion of the micritic calcite. Furthermore, the lamination can be a consequence of seasonal rhythmic growth; the spring bands are darker and thinner [24]. Some large irregular cavities (2 × 1 mm in size) appear as organic structures of plants that were associated to travertine deposition. Large cavities may be filled by mosaic calcite of secondary origin [26,41].

These cavities were observed also by means of ESEM allowing discernment of pore gradation (pores from 4 μm up to 700 μm) and irregular abrasion of calcite crystals in the polished surface. The abrasion can be interpreted as a result of mechanical polishing of the stone, where calcite crystals were unpinned from the stone surface thus favouring the differential erosion of the stone surface. Moreover, the uneven abrasion could be enhanced by the different crystals sizes, as well as by their different crystallographic orientation – on the stone surface – that could generate asymmetrical decay [42].

3.2.4. Pore system

Table 3 shows the porosimetric parameters of fresh rough and polished travertine samples determined by MIP. The mean open porosity for rough fresh samples was ~8.16% characterising AL travertine as a medium porous stone. After the polishing process this value slightly decreased to ~7.26%, a fact attributed to the filling process with the resin used in the polishing process. Fig. 4a and b shows the pore size distribution obtained by means of MIP for rough and polished freshly quarried samples. Both curves are bimodal and strongly asymmetric. The main pore size range for the rough surface is comprised between 0.02 and 0.07 μm (radius size) with a secondary peak centred at 100 μm (Fig. 4a). By contrast the polished travertine displays a pore size distribution where the main peak is centred at 100 μm and the secondary peak appears in the range of 0.02–0.05 μm (Fig. 4b). The decrease of the main pore size range could be assigned to the sealing effect of the resin used to improve the stone endurance during polishing. Moreover, the increase of pores centred at ~100 μm could be related to the induced stone damage during the polishing process (small detached crystal grains can scratch the stone surface) as well as to small bubbles or defects inherent to the resin used to fill travertine voids.

Ar sorption was applied to investigate the smallest pore sizes of fresh polished and non-polished samples (Fig. 5 and Table 4). Representative Ar sorption isotherms of these samples are shown in

Table 3
Mercury intrusion porosimetry parameters: n_0 = open porosity (%); ρ_A = apparent (skeletal) density (g cm^{-3}); ρ_B = bulk density (g cm^{-3}).

Surface	Type	n_0	ρ_A	ρ_B
Rough	Fresh	8.16 ± 1.21	2.65 ± 0.04	2.43 ± 0.04
	Aged	10.65 ± 0.57	2.70 ± 0.06	2.48 ± 0.06
Polished	Fresh	7.26 ± 0.25	2.66 ± 0.04	2.42 ± 0.01
	Aged	8.34 ± 0.93	2.70 ± 0.03	2.49 ± 0.01

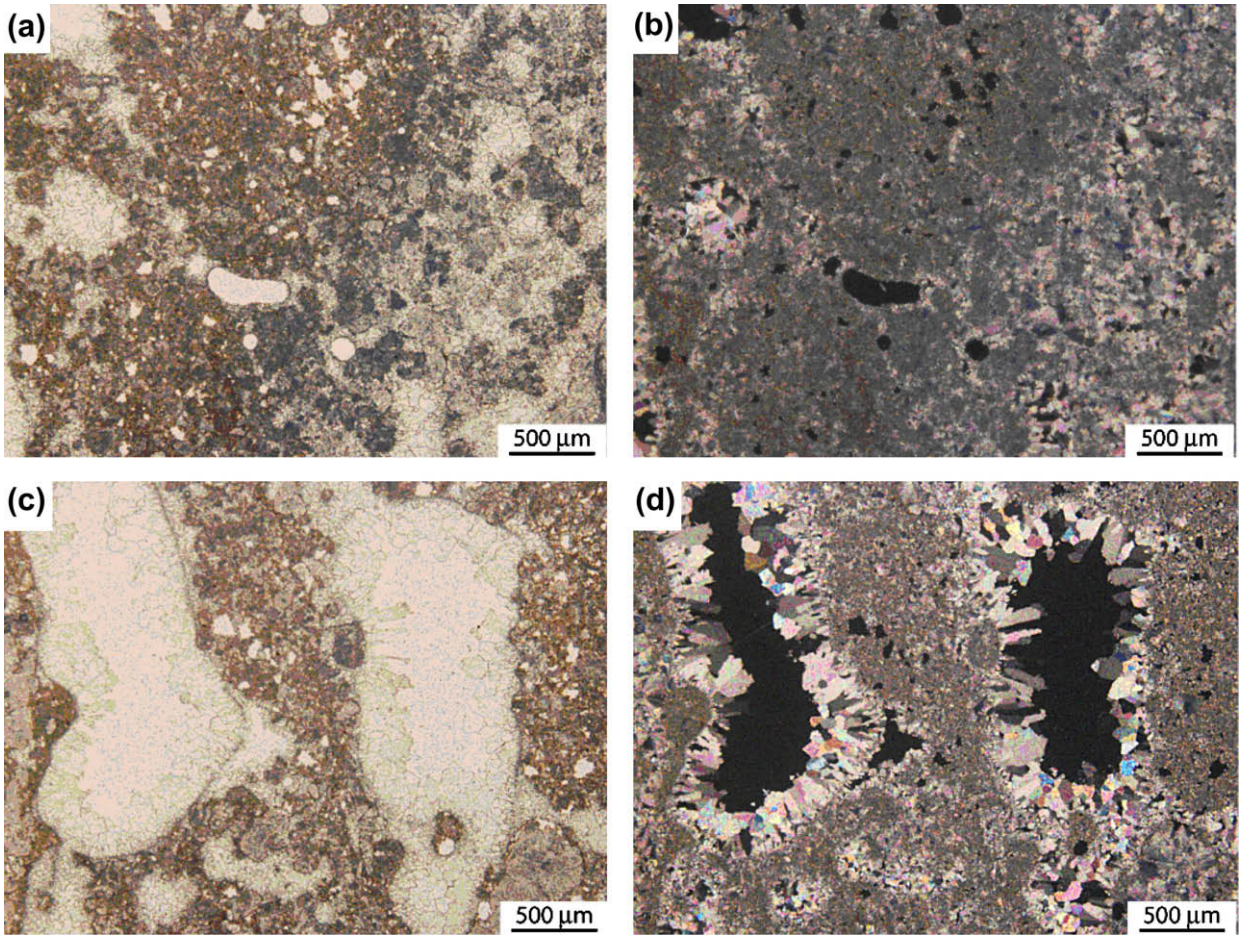

Fig. 3. Optical microphotographs showing the representative textures of freshly quarried travertine stained with red alizarin: (a) colour layering due to contrasting sparitic and micritic calcite content (parallel polarised light) (b) same as (a) under crossed polarised light where sparitic calcite (right) is clearly observed (c) detail of irregular and elongated pores (2 × 1 mm in size) under parallel polarised light (d) pores are incompletely filled by coarse grain sparitic calcite (>150 μm) (crossed polarised light). (For interpretation of the references to colour in this figure legend, the reader is referred to the web version of this article.)

Table 4
Pore system characteristics determined by Ar sorption (BET) of samples with rough and polished surface before and after the ageing test.

	Fresh samples		Aged samples	
	Rough surface	Polished surface	Rough surface	Polished surface
Surface area (BET) (m^2/g)	0.5601 ± 0.1042	0.2387 ± 0.0853	0.9133 ± 0.2789	0.2245 ± 0.0193
Total pore volume (cm^3/g)	0.00037 ± 0.00007	0.00022 ± 0.00007	0.00076 ± 0.00007	0.00022 ± 0.00007
Average pore diameter (Å)	20.53 ± 1.48	20.60 ± 0.75	20.64 ± 0.74	21.07 ± 1.42
Monolayer volume	0.1468 ± 0.0270	0.0624 ± 0.0363	0.2394 ± 0.0739	0.0589 ± 0.0050
Surface fractal dimension (D_S)	2.52	2.51	2.54	2.51
Linear correlation coefficient (r^2)	0.9974	0.9912	0.9978	0.9934

Reported values are the mean and standard deviation of three measurements.

Table 5
Mean values and standard deviation of chromatic parameters and their variations in travertine samples before and after the test, and after mechanical and distillate water cleaning of salts from the stone surface.

Surface	Type	L^*, mean	a^*, mean	b^*, mean	C^*, mean	H^*, mean	ΔL^*	Δa^*	Δb^*	ΔC^*	ΔE^*
Rough	Fresh	69.78	1.83	7.31	7.54	75.9					
	Aged	77.04	1.31	3.17	3.43	67.6	7.26	−0.53	−4.14	−4.11	8.38
	Rasped	80.13	1.16	2.96	3.18	68.6	10.35	−0.67	−4.35	−4.36	11.25
	Washed	79.78	1.24	2.89	3.15	66.7	10.00	−0.59	−4.42	−4.39	10.95
Polished	Fresh	62.00	5.52	15.69	16.63	70.6					
	Aged	71.20	2.69	8.47	8.89	72.4	9.20	−2.83	−7.22	−7.75	12.03
	Rasped	78.31	2.64	9.54	9.90	74.5	16.31	−2.88	−6.15	−6.73	17.67
	Washed	79.35	2.07	9.07	9.30	71.15	17.35	−3.45	−6.62	−7.33	18.89

L^* brightness; a^* red–green components; b^* yellow–blue components; C^* chroma, $C^* = \sqrt{(a^*)^2 + (b^*)^2}$; H^* hue; $\Delta E^* = \sqrt{(\Delta L^*)^2 + (\Delta a^*)^2 + (\Delta b^*)^2}$.

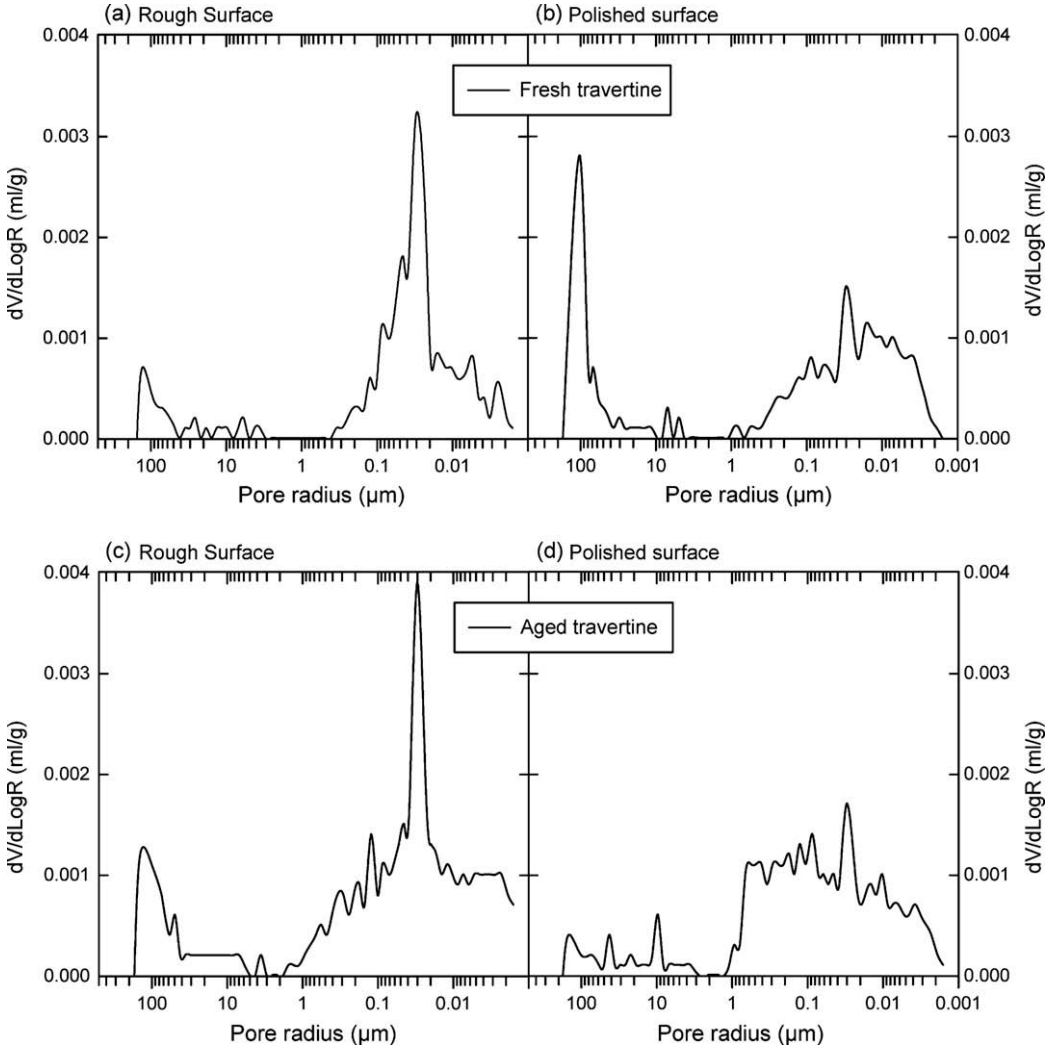

Fig. 4. Pore size distribution measured by MIP of freshly quarried travertine with rough (a) and polished (b) surface. Note that the main pore size range for (a) is comprised between 0.02 and 0.07 μm (radius) whereas in (b) is centred at 100 μm. Pore size distribution after the sea-salt spray test for the aged travertine with rough (c) and polished (d) surface.

Fig. 5a and b. Both isotherms are of type II [32] and indicate the non-microporous nature of these samples; this is further confirmed by the very low surface area, i.e. 0.5601 ± 0.1042 m^2/g vs. 0.2387 ± 0.0853 m^2/g respectively for rough and polished travertine samples (Table 4). Table 4 also shows that the porosity of both travertine types is concentrated in the mesopore range, with an average pore diameter of 20.53 ± 1.48 Å for the rough surface and 20.60 ± 0.75 Å for the polished surface.

Finally, the BJH plots (pore size distribution curves named after Barret–Joyner–Halenda) are almost equivalent (Fig. 5c and d). Total pore volume is lower in polished samples than in rough ones (due to filling with resin as explained above), although the complexity of the pore system expressed as the surface fractal dimension (D_S = 2.52 vs. D_S = 2.51 for rough and polished samples respectively) is virtually similar (Table 4).

3.2.5. Colourimetry

The study of the chromatic characteristics presented in Table 5 showed that the polishing process of the travertine caused a decrease of the brightness parameter L^* (*69.78* vs. 62.00) and an increase of the chromatic parameters a^* (*1.83* vs. 5.52) and b^* (*7.31* vs. 15.69). This means that after polishing the travertine becomes more reddish and yellowish.

3.3. Aged samples

3.3.1. Macroscale observations

During the sea-salt ageing test no stone detachments were observed. The first efflorescences crystallised as crusts after 48 h exposure into the test chamber in all samples, most profusely in the rough ones. Salt crusts started to grow at the upper borders of each tablet and afterwards extended and covered the tablets completely (Fig. 6). The weight of all samples increased slightly after the test (0.65% for rough travertine and 0.60% for polished travertine). The salt crusts were thicker in the polished travertines.

3.3.2. Mineralogical and textural characteristics

Halite (NaCl) was the only salt detected by means of XRD. No other minority phases (detectable at 5% or more) as for example sulphates – detected in the seawater used in the test, see Table 1 – were found by XRD.

Detailed OM observations of the aged samples revealed no important microtextural differences, neither between fresh and aged travertine nor between rough and polished surfaces. In some parts of the aged rough samples a slight reduction of the sparitic calcite that covered the cavities was observed. In addition it was

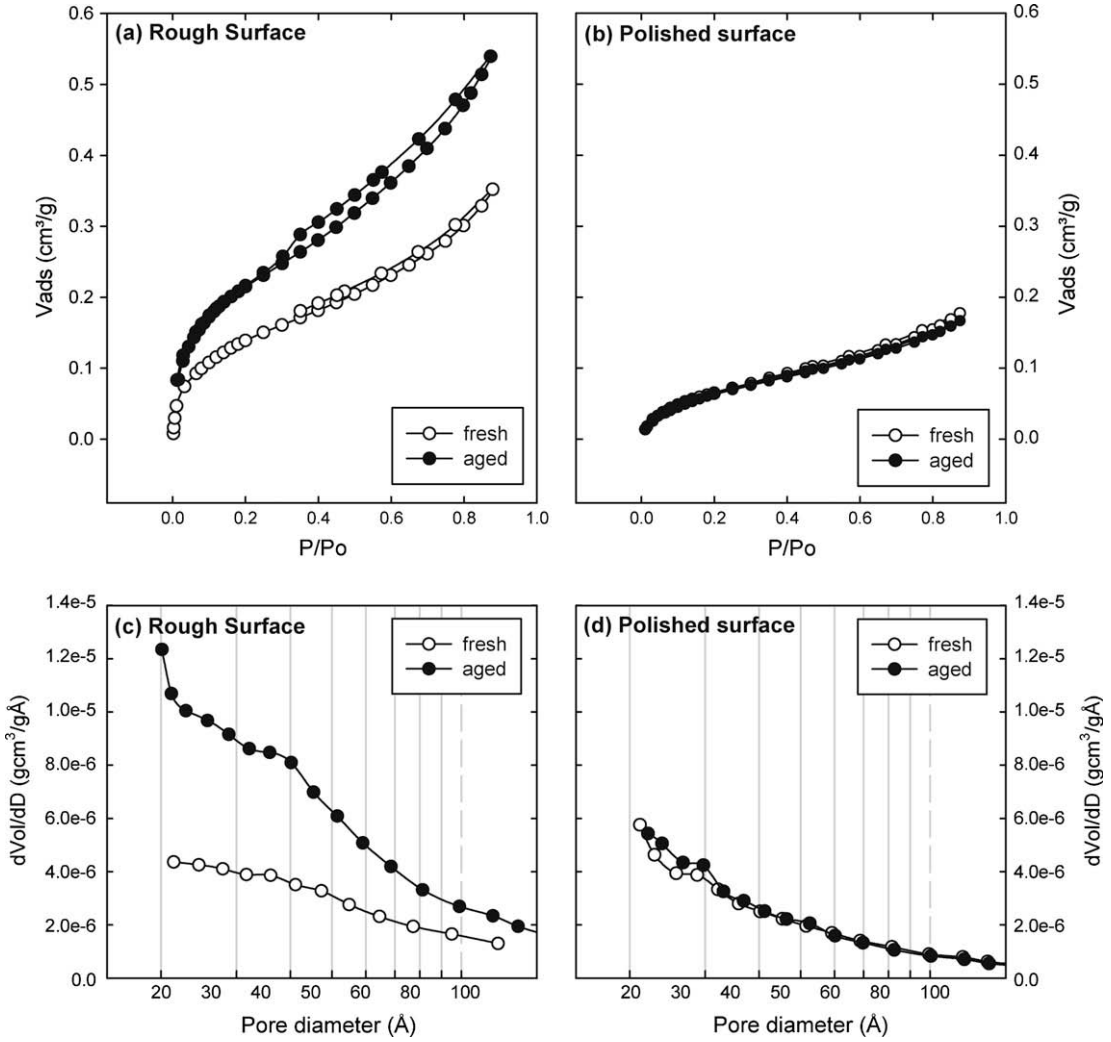

Fig. 5. Ar (−196 °C) physisorption isotherms for fresh (empty dots) and aged (filled dots) travertine with rough (a) and polished (b) surface. BJH pore size distribution plot of Ar physisorption curve for fresh (empty dots) and aged (filled dots) travertine samples with (c) rough and (d) polished surface.

confirmed that the marine aerosol affected only the most superficial part (first 200 μm) of the stone samples.

By ESEM small unconnected and discontinuous salt crusts of xenomorphic or anhedral halite crystals (no crystal faces present) formed in the rough travertine were observed (Fig. 7a). These crusts partially covered original coarse-grained calcite crystals. Crystalline habits formed in polished travertine surfaces were more diverse since homogeneous and continuous halite crusts developed (Fig. 7b). In fact, four crystalline habits of halite could be recognised (Fig. 7c): (1) small subhedral crystals (some faces present); (2) dendritic crystals (with a typical multi-branching tree-like form) with a hole in the centre (*hopper* crystals); (3) transition into oblong (column) crystals with scarce holes and (4) crystals that tend to form cubes (50–100 μm in size) in the upper part of the crust, where desiccation fissures were observed. This sequence suggests a change in the supersaturation of the saline solution which promotes the halite crystallisation. While the presence of abundant small subhedral and dentritic crystals are indicative of high growth rates and supersaturation values, the development of *hopper* and cubic crystals in this test suggests stable growth at medium/low supersaturation in last crystallisation stages [17,43–45].

Furthermore, pseudo-hexagonal tabular crystals of gypsum were locally identified in the polished stone surface (Fig. 7d). It should be recalled that gypsum was present in the plaster used in the polishing process, thus it is possible that gypsum crystals appear after the salt ageing test on the polished travertine. However the observed morphology is not typical of gypsum which crystallised in the monoclinic system. It has been reported that pedogenic gypsum can exhibit diverse crystal morphologies that may be controlled by a variety of environmental conditions including pH, temperature, salinity, organic matter and clays. In particular, tabular pseudo-hexagonal gypsum crystals (like those observed in this study) have been associated with organic matter and microorganisms [46]. Already these specific conditions can be attained in this work via the organic matter and microorganisms present during the travertine formation and those possibly contained in the seawater used in the test.

3.3.3. Pore system

The modification of the pore system due to the salt ageing test differs for rough and polished samples (Table 3). In rough samples the increase of the open porosity was higher (from ~8.16% toward ~10.65%) compared to the polished samples (from ~7.26% towards ~8.34%). Nonetheless no important modifications of the pore size distribution occurred as shown in Fig. 4, although a slight increase of the pore volume for all pore sizes was observed compared to the fresh travertine samples.

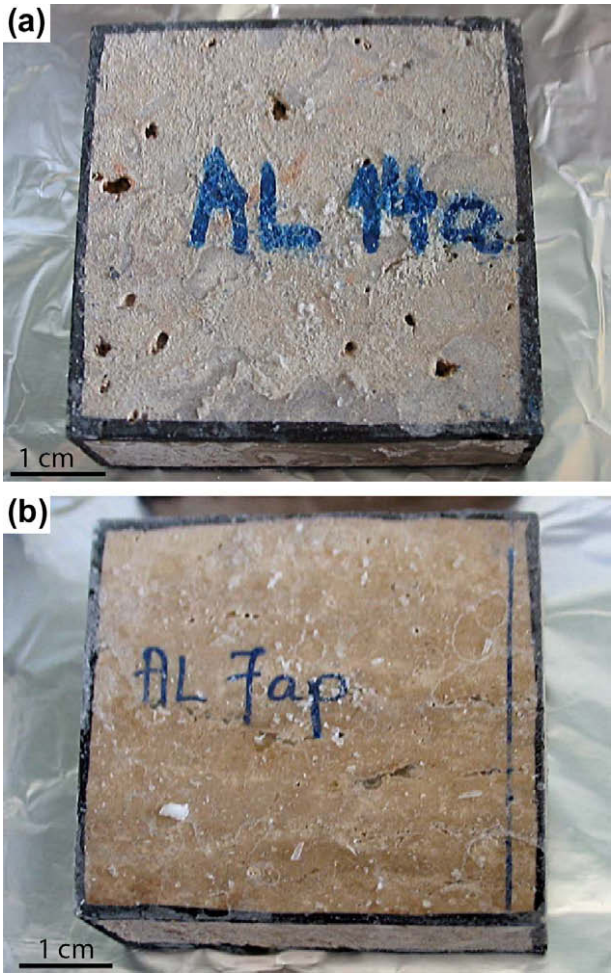

Fig. 6. Macroscopic features of the aged travertine with rough (a) and polished (b) surface after the sea-salt ageing test.

In other carbonate stones as for instance limestone several authors have observed a decrease of the open porosity after diverse salt crystallisation tests, which was attributed to pores infilling by salts [9,17,19]. In the samples of this work, the slight increase in the open porosity could be related either to the textural heterogeneity of this type of travertine or to (chemical) dissolution processes. In fact, the small increase in pores around 100 μm (Fig. 4c) could be justified by dissolution of the calcite that refills pores of such size, as confirmed by OM and ESEM. Calcite cement dissolution due to the action of marine aerosols on limestones placed in monuments has already been reported elsewhere [2]. Additionally, the open fabric of the studied travertine could have enhanced the salt spray attack stimulate by the surface roughness.

On the contrary the small increase in the open porosity of the polished samples (~7.26% vs. ~8.34%, Table 3) falls within the measurement error, and suggests that these stones were less deteriorated by the marine spray than the non-polished stones. When comparing Fig. 4b and d it is observed that after the test, pores around 100 μm almost disappeared, which is attributed to infilling with salts, while pores between 0.001 and 1 μm remained essentially unaffected (see Fig. 4b vs. Fig. 4d). The study of the aged polished travertine with ESEM and the Ar sorption analysis (regarding the pore system modification explained below) already confirmed the minor alterations that took place in the polished samples after the salt spray test.

The different behaviour of both surface finishings in response to the sea-salt spray action was particularly highlighted by the modification of pores (1–100 nm) analysed with Ar sorption. As shown in Fig. 5a a significant increase of the isotherm slope for the rough samples after the test occurred. It is known that roughness and complexity of the surface define the isotherm slope, which can be further related to the surface fractal dimension [47–49]. Salt crystallisation inside stones causes an increase of both roughness and surface complexity, which leads to an increase in the fractal dimension (D_S) values. Conversely, crack opening and widening produce a decrease of D_S [49]. In this work the significant increase of the isotherm slope of the aged travertine (Fig. 5a) gives rise to an increase of the fractal dimension compared to that of the fresh travertine (D_S^{fresh} = 2.52 vs. D_S^{aged} = 2.54, Table 4). Calcite dissolution induced by salt crystallisation may account the increase of the fractal dimension [50]. Increase of fractal dimension can be used to estimate damage degrees of a material [51]. In this work, this damage degree was also confirmed by the large increase of the total pore volume for the rough travertine samples after the test as shown in Table 4 (i.e. ~0.00037 vs. ~0.00076 cm^3/g before and after the test respectively). The total pore volume increase can be related to the crack opening and chemical attack produced during the salt ageing test.

In contrast to rough samples, no changes of the isotherm adsorption slope were observed for polished aged samples (Fig. 5b). Therefore, the fractal dimension remained constant after the ageing test owing to the protecting effect of the resin ($D_S^{fresh} = D_S^{aged}$ = 2.51, Table 4). Similarly, total pore volume and surface area did not change (Table 4) and values were below those of rough samples, showing that the resin also filled pores with radius below than 50 nm. All these results indicate that the pore system characteristics measured by Ar sorption were not modified after the sea-salt ageing test.

3.3.4. Colourimetry

Chromatic parameters of the rough and polished aged travertine surfaces were determined using the following approach: (1) measurements on surfaces covered by salt crusts, (2) measurements on surfaces where efflorescences were mechanically removed and (3) measurements on aged stone surfaces washed in distillate water during one week. The second and third approach can be useful to evaluate the efficiency of cleaning interventions to recuperate the original stone chromatic characteristics. Table 5 shows the chromatic parameters of all the studied samples (these are average values of three measurements for each sample and their standard deviations). Perceptible visual changes are achieved only when ΔE^* (total colour difference = $\sqrt{(\Delta L^*)^2 + (\Delta a^*)^2 + (\Delta b^*)^2}$) exceeds three units. Thus colour alterations were observed for all aged samples, particularly in the polished samples and more precisely in those where salts were mechanically removed, i.e. ΔE^* = 17.67 (Table 5).

Furthermore, after the ageing test and elimination of salt crusts the ΔL^* (brightness difference) was higher in polished samples than in rough ones (10.35 vs. 16.31, Table 5) (Fig. 8a). Moreover, the alteration caused all samples to become more green and blue (cold tones) as parameters a^* and b^* decreased (Table 5).

Chromatic parameter variations related to the fresh travertine can be quantified together by means of chroma differences. Fig. 8b shows the decrease of chroma after the ageing test which remained nearly constant after mechanical cleaning of the surface. Interestingly the development of salt cleavage planes during the surface rasping caused a luminosity increase in both rough and polished samples (Fig. 8a). Moreover chroma and brightness differences remained constant after surface cleaning with distillate water indicating that the chromatic effect of the salt damage is irreversible (Fig. 8a and b).

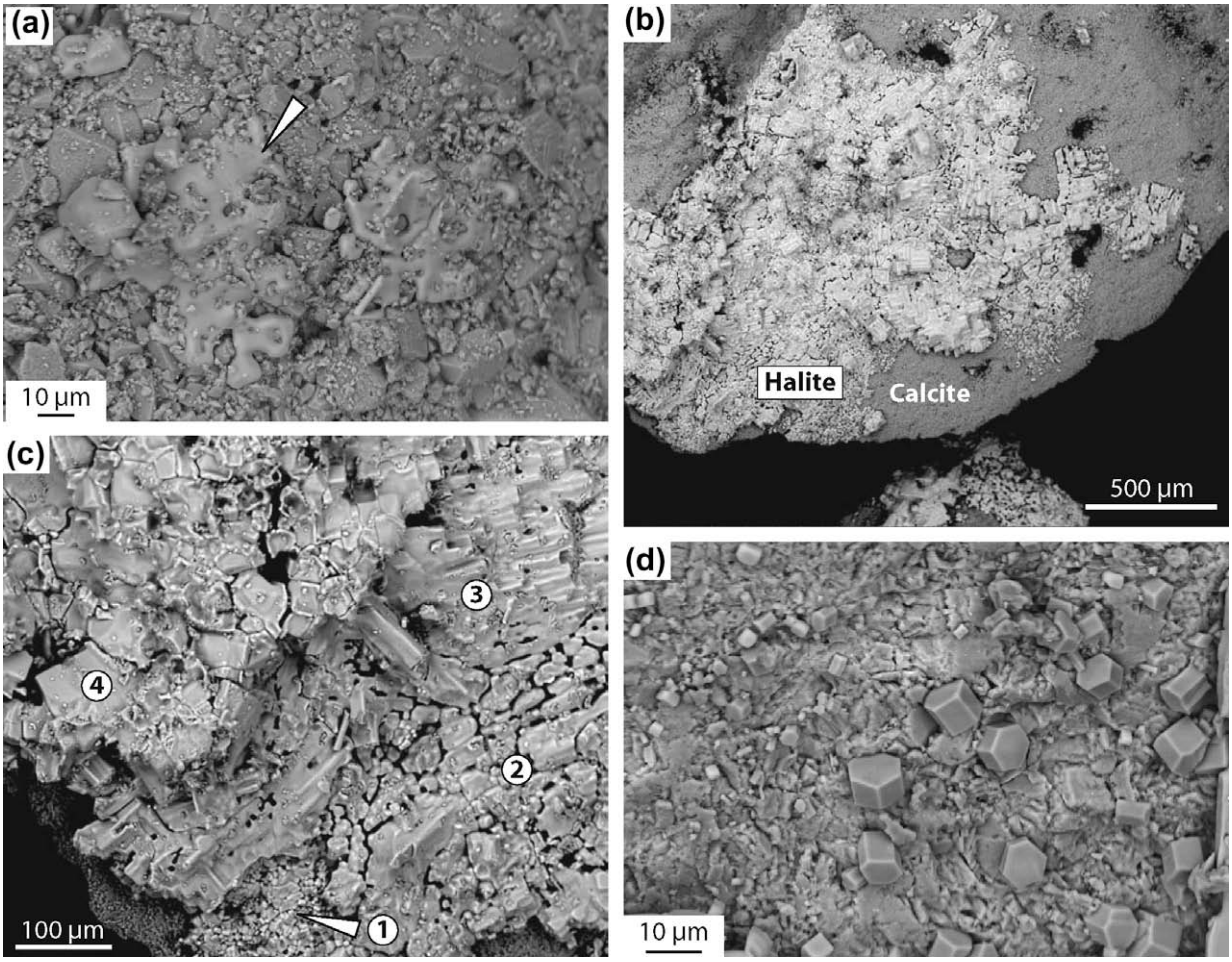

Fig. 7. Electron backscattered images of the aged travertine with (a) rough surface where coarse sparitic calcite is covered by thin xenomorphic halite crust (arrow) (b) polished surface where halite crystals form a thick (>2 mm) homogeneous crust with dendritic textures indicating medium to high supersaturation (c) detail of these crusts where up to four different halite textures can be distinguished (see text for the explanation) and (d) pseudo-hexagonal gypsum crystals on the polished surface of travertine.

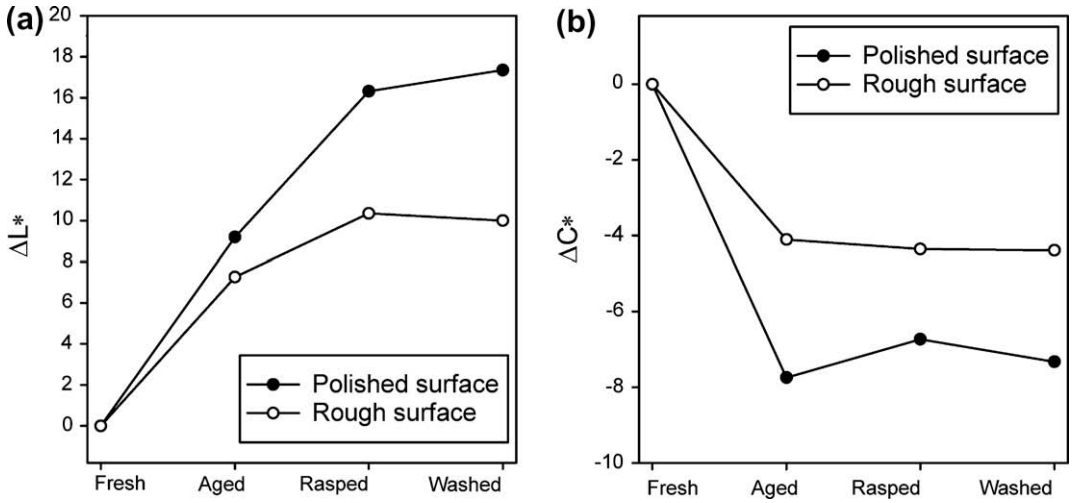

Fig. 8. Changes in the chromatic parameters of the travertine with rough (empty dots) and polished surface (filled dots) between fresh samples, aged ones and aged samples after salt cleaning: (a) variation of brightness (ΔL^*) and (b) variation of chroma (ΔC^*).

4. Conclusions

Results from a realistic sea-salt spray test on the massive *Olivillo travertine* (Southern Spain) have revealed that stone damage due to the impact of marine aerosols is strongly related to the stone surface finishing (i.e. rough or polished surface stone). In fact, the polished finishing – combined with a gypsum-based plaster and an epoxy silicone resin infilling – protects the travertine against

marine salt corrosion. On the basis of surface fractal dimension analyses, it is clear that this finishing process effectively blocks the pore system in the near-surface zone of the travertine, thus preventing penetration of the saline spray into the stone. By contrast, on the irregular rough travertine surface, salt crystallisation is more abundant and induces larger open porosity and also greater surface fractal dimension than in the polished stones, which in turn make it more vulnerable to further salt spray attack.

Apart from this, in terms of chromatic alteration, on rough surfaces chromatic changes are less intense than on polished stones. In fact, the latter become brighter and lose their valued warm tonality, since chromatic parameters were found to be displaced toward more blue and green values. Therefore, salt cleaning interventions based on mechanical removal of efflorescences are not advisable.

This study emphasises that prior to establishing conservation or maintenance practices, it is advisable to characterise the materials used in filled travertines (as well as in other stone types), since undesirable products such as gypsum salt can activate weathering mechanisms. Also, in coastal areas it is recommended to apply *ad hoc*, long-term salt-spray ageing tests on construction and decorative materials to optimise conservation interventions for buildings exposed to marine aerosols.

Acknowledgements

Financial support for this work was provided by the Andalusian Research Group RNM-179, Research Project FTQ-1633 and a research contract from the *Junta de Andalucía* awarded to C. Cardell. We thank C. Rodríguez-Navarro for valuable revision suggestions, J. Romero and P. Alvarez for FTIR spectroscopy interpretation and A. Kowalski for English revision. M. Urosevic is supported by a fellowship from the Spanish Science Ministry (AP2006-036).

References

[1] Anwar Hossain KM, Easa SM, Lachemi M. Evaluation of the effect of marine salts on urban built infrastructure. Build Environ 2009;44:713–22.
[2] Cardell C, Delalieux F, Roumpopoulos K, Moropoulou A, Auger F, Van Grieken R. Salt-induced decay in calcareous stone monuments and buildings in a marine environment in SW France. Constr Build Mater 2003;17:165–79.
[3] Mottershead D, Gorbushina A, Lucas G, Wright J. The influence of marine salts, aspect and microbes in the weathering of sandstone in two historic structures. Build Environ 2003;38:1193–204.
[4] Stefanis N-A, Theoulakis P, Pilinis C. Dry deposition effect of marine aerosol to the building stone of the medieval city of Rhodes, Greece. Build Environ 2009;44:260–70.
[5] Charola AE. Salts in the deterioration of porous materials: an overview. J Am Inst Conserv 2000;39:327–43.
[6] Doehne E. Salt weathering: A selective review. In: Siegesmund GS, Vollbrecht A, Weiss T, editors. Natural stone, weathering phenomena, conservation strategies and case studies. London: Geological Society; 2003. p. 205–19.
[7] Benavente D, García del Cura MA, Bernabeu A, Ordóñez S. Quantification of salt weathering in porous stones using an experimental continuous partial immersion method. Eng Geol 2001;59:313–25.
[8] Cardell C, Rivas T, Mosquera MJ, Birginie JM, Moropoulou A, Prieto B, et al. Patterns of damage in igneous and sedimentary stones under conditions simulating sea-salt weathering. Earth Surf Process Land 2003;28:1–14.
[9] Cardell C, Benavente D, Rodríguez Gordillo J. Weathering of limestone building material by mixed sulfate solutions. Characterization of stone microstructure, reaction products and decay forms. Mater Charact 2008;59(10):1371–85.
[10] Rivas T, Prieto B, Silva B, Birgine JM, Auger F. Comparison between traditional and chamber accelerated ageing tests on granitic stones. In: Proceedings of 9th international congress on deterioration and conservation of Stone, Venice, 2000. p. 171–80.
[11] Rivas T, Prieto B, Silva B, Birginie JM. Weathering of granitic stones by chlorides: effects of the nature of the solution on weathering morphology. Earth Surf Process Land 2003;28:425–36.
[12] Rodriguez-Navarro C, Doehne E. Salt weathering: influence of evaporite rate, supersaturation and crystallisation pattern. Earth Surf Process Land 1999;23(3):191–209.
[13] ASTM B-117: Standard practice for operating salt spray (fog) apparatus. Philadelphia: Am Soc Testing Mater; 1997.
[14] DIN 50021: spray tests with different sodium chloride solutions. In: Normung EV, editor. Deutsches Institut für. German National Standard; 1988.
[15] ISO International Organization for Standardization. ISO 9227, Corrosion tests in artificial atmospheres – salt spray tests; 2006.
[16] UNE-EN 14147: natural stone test methods. Determination of resistance to ageing by salt mist. Madrid: Spanish Association for Standardisation and Certification (AENOR); 1994.
[17] Cardell C. Cristalización de sales en calcarenitas. Aplicación al Monasterio de San Jerónimo, Tesis Doctoral. Granada: University of Granada, Faculty of Science, Department of Mineralogy and Petrology; 1998.
[18] Steiger M, Zeunert K. Crystallisation properties of salt mixtures: comparison of experimental results and models calculations. In: Proceedings of 8th international congress on deterioration and conservation of stone, Berlin, 1996. p. 535–44.
[19] Ruiz-Agudo E, Mees F, Jacobs P, Rodríguez-Navarro C. The role of saline solution properties on porous limestone salt weathering by magnesium and sodium sulfates. Environ Geol 2007;52:269–81.
[20] Pentecost A. The quaternary travertine deposits of Europe and Asia Minor. Quater Sci Rev 1995;14:1005–28.
[21] Ford TD, Pedley HM. A review of tufa and travertine deposits of the world. Earth Sci Rev 1996;41:117–75.
[22] Török Á. Influence of fabric on the physical properties of limestones. In: Kourkoulis SK, editor. Fracture failure of natural building stones. Applications in the restoration of ancient monuments. Dordrecht: Springer-Verlag; 2006. p. 487–97.
[23] Durán-Suárez JA, García-Casco A, Sánchez-Navas A, Rodríguez-Gordillo J. Caracterización de las alteraciones en pilares de travertino de la Iglesia del Salvador (Granada). Propuestas restauradoras. Bol Soc Esp Miner 1993;16:1–12.
[24] Gauri K, Bandyopadhyay JK. Carbonate stone chemical behavior durability and conservation. New York: J. Wiley & Sons; 1999.
[25] Demirdag S. The effect of using different polymer and cement based materials in pore filling applications on technical parameters of travertine stone. Constr Build Mater 2009;23:522–30.
[26] Török Á. Surface strength and mineralogy of weathering crusts on limestone buildings in Budapest. Build Environ 2003;38:1185–92.
[27] Török Á. Black crusts on travertine: factors controlling development and stability. Environ Geol 2008;56:583–94.
[28] Voersman F, Baena J. Mapa geológico de España escala 1:50.000. Hoja 1.044 Alhama de Almería. Mapa y memoria. Madrid: Geological and Mining Institute of Spain (IGME); 1983.
[29] García del Cura MA, Sanz-Montero E, Benavente D, Martínez-Martínez J, Bernabéu A, Cueto N. Sistemas travertínicos de Alhama de Almería: características petrográficas y petrofísicas. Geotemas 2008;10:456–9.
[30] García del Cura MA, La Iglesia A, Ordóñez S, Sanz-Montero E, Benavente D. Óxidos de hierro y manganeso en travetinos de Alhama de Almería. Macla 2008;9:107.
[31] Martín Ramos JD. XPowder: a software package for powder X-ray diffraction analysis. Granada: Lgl. Dep. GR 1001/04; 2004.
[32] Sing KSW, Everett DH, Haul RAW, Moscou L, Pierotti RA, Rouquérol J, et al. Reporting physisorption data for gas/solid systems with special reference to the determination of surface area and porosity (recommendations 1984). Pure Appl Chem 1985;57:603–19.
[33] Gregg SJ, Sing KSW. Adsorption surface area and porosity. London: Academic Press; 1982.
[34] Adamson AW, Gast AP. Physical chemistry of surfaces. New York: J. Wiley & Sons; 1997.
[35] Barret EP, Joyner LG, Halenda PP. The determination of pore volume and area distributions in porous substances I. Computations from nitrogen isotherms. J Am Chem Soc 1951;73:373–80.
[36] Tang P, Chew NJK, Chan H-K, Raper JA. Limitation of determination of surface fractal dimension using N_2 adsorption isotherms and modified Frenkel–Halsey–Hill theory. Langmuir 2003;19:2632–8.
[37] Wyszecki G, Stiles WS. Colour science. Concepts and methods, quantitative data and formulae. 2nd ed. New York: J. Wiley & Sons; 1982.
[38] Andersson J, Hillborg H, Gubanski SM. Deterioration of internal interfaces between silicone and epoxy resin. In: Conference record of the 2006 IEEE international symposium on electrical insulation; 2006. p. 527–30.
[39] Crnkovic B, Poggi F. Travertine the restoration stone for the Zagreb Cathedral. Mining Geol Petrol Eng Bull 1995;7(1):77–85.
[40] Petrelli M, Perugini D, Moroni B, Poli G. Determination of travertine provenance from ancient buildings using self-organizing maps and fuzzy logic. Appl Artif Intell 2003;17:885–900.
[41] Pentecost A. Travertine. Berlin Heidelberg: Springer-Verlag; 2005.
[42] Rodríguez-Navarro C, Rodríguez-Navarro A, Elert K, Sebastián E. Role of marble microstructure in near-infrared laser-induced damage during laser cleaning. J Appl Phys 2004;95:3350–7.
[43] Sunagawa I. Characteristics of crystal growth in nature as seen from the morphology of mineral crystals. Bull Minéral 1981;104:81–7.
[44] Rodriguez-Navarro C, Doehne E, Sebastián E. How does sodium sulfate crystallize? Implications for the decay and testing of building materials. Cem Concr Res 2000;30:1527–34.
[45] Markov I. Crystal growth for beginners. Fundamentals of nucleation, crystal growth and epitaxy. 2nd ed. Singapore: World Scientific Publishing Company; 2003.
[46] Buck BJ, Van Hoesen JG. Snowball morphology and SEM analysis of pedogenic gypsum, Southern New Mexico, USA. J Arid Environ 2002;51:469–87.

[47] Avnir D, Jaroniec M. An isotherm equation for adsorption on fractal surfaces of heterogeneous porous materials. Langmuir 1989;5(6):1431–3.
[48] Lefebvre Y, Lacelle S, Jolicoeur C. Surface fractal dimensions of some industrial minerals from gas-phase adsorption isotherms. J Mater Res 1992;7:1888–91.
[49] Ruiz-Agudo E, Luque A, Sebastián EM, Rodríguez-Navarro C. Changes in the pore structure of marble after salt decay tests. In: Proceedings of 9th international congress on heritage and building conservation, Seville, 2008. p. 153–8.
[50] Ruiz-Agudo E, Putnis CV, Jiménez-López C, Rodriguez-Navarro C. An atomic force microscopy study of calcite dissolution in saline solutions: The role of magnesium ions. Geochim Cosmochim 2009;73:3201–17.
[51] Xie H, Wang J, Qan P. Fractal characters of micropore evolution in marbles. Phys Lett A 1996;218:275–80.